Applied Radiation and Isotopes 176 (2021) 109854

Contents lists available at ScienceDirect

Applied Radiation and Isotopes

journal homepage: www.elsevier.com/locate/apradiso

Gamma-ray spectroscopy with anode pulses of NaI(Tl) detector using a low-cost digitizer system

Hadi Kasani [a,*], Saleh Ashrafi [a], Nima Ghal-Eh [b], Hector Rene Vega-Carrillo [c]

[a] Faculty of Physics, University of Tabriz, Tabriz, Iran
[b] Department of Physics, Faculty of Science, Ferdowsi University of Mashhad, P.O. Box 91775-1436, Mashhad, Iran
[c] Unidad Academica de Estudios Nucleares, Universidad Autonoma de Zacatecas, Cipres 10, Fracc. La Penuela, 98068, Zacatecas, Mexico

ARTICLE INFO

Keywords:
COTS digitizer
Gamma-ray spectrometry
NaI detector
Pile-up correction

ABSTRACT

Recently, digital gamma-ray spectroscopy employing low-cost and publicly available (Commercial off the shelf) digitizers has been frequently used in different studies worldwide. In this paper, we considered the digital methods for gamma-ray spectroscopy in which the anode pulses of the photomultiplier tube (PMT) output in a NaI(Tl) scintillation detector were immediately digitized by a PC sound card. We introduced and developed the methods for gamma-ray spectroscopy of microCurie gamma-ray sources by a sampling rate of 96 kHz. First, at low count rates, the pulse arrival time was determined directly by the raw waveform, and the gamma-ray spectrum was obtained by summing the corresponding values in the samples per pulse. In addition, the gamma-ray spectrum was obtained by an enhanced sampling rate waveform and the pulse arrival time was determined by employing the digital constant fraction discrimination (DCFD) method, where each pulse area was achievable by summing the corresponding values of pulse samples. On the other hand, fitting the appropriate model function on the pulses and obtaining the fitted pulse area were undertaken for gamma-ray spectroscopy. To this end, a non-iterative algorithm to fast fit the Gaussian model function was improved. Moreover, the pile-up correction was performed at different count rates employing the Maximum Likelihood Estimation (MLE) method and Gaussian model function. Also, an approximate method for solving the high run time challenge was identified in the MLE method for long-time waveforms. To reject the pile-up events, a method was introduced based on the calculation of the full-width at half maximum pulses. By applying the proposed rejection method, we achieved an energy resolution of 6.2% at 663 keV gamma-rays and a count rate of 5.3 kcps.

1. Introduction

Gamma-ray spectroscopy is widely applied in the industry (Mantero et al., 2015), medicine (Kinahan and Karp, 1990), and radiation-related sciences. With the advent of fast digitizers equipped with powerful processors, methods of digital analysis of gamma-ray detector outputs have become more diverse and important (Buzzetti et al., 2005). Commercially available digitizers (Commercial off the shelf) are used (Huang and Jiang, 2018), because of their low cost and easy installation. Nowadays, in all electronic communication and business devices (e.g., personal computers, laptops, tablets, or smartphones), there is a mechanism for storing and transmitting sounds. This task is carried out with sound cards where the sound waves are digitalized and processed. In this work, we directly digitized the output anode pulses of a NaI(Tl) detector using a personal computer (PC) sound card, and developed optimizing algorithms to obtain the Cs-137 gamma-ray pulse-height spectrum.

Basically, the anode pulses from the PMT carry information about the gamma-ray energy such that the pulse area represents the corresponding gamma-ray energy (Knoll, 2010). The main destructive effect at high count rate gamma-ray spectroscopy is the pulse pile-up; where the second pulse arrives on the tail of the first pulse, the second pulse area cannot correspond to the gamma-ray energy. This effect must be eliminated as often as possible using the so-called pile-up correction algorithms (Mohammadian-Behbahani and Saramad, 2020). Note should be taken that the elimination of pile-up events when sound cards are used is not favorable in high-efficiency applications, since they have a low sampling rate, where each pulse is limited to 3 or 4 samples. In that case, it was difficult to correct the effect of pile-up events on the energy spectrum obtained by a raw waveform. Because the general shape of the anode pulses was stable, the methods for detection, correction, and

* Corresponding author.
E-mail address: hadi.kasani@tabrizu.ac.ir (H. Kasani).

https://doi.org/10.1016/j.apradiso.2021.109854
Received 25 April 2021; Received in revised form 2 June 2021; Accepted 30 June 2021
Available online 4 July 2021

rejection of pile-up events were presented in this work (Knoll, 2010).

The determination of the arrival time and a suitable length for the waveform pulses are essential for the pulse area calculation (i.e., the gamma-ray energy determination). Besides, the selection of an appropriate pulse model function is important for the digitized anode pulses. The model function being selected, the energy value of each gamma-ray, and the subsequent energy spectrum of the corresponding gamma-ray source were achievable by fitting the model function on the obtained pulses from a waveform.

In this paper, the arrival time of the pulses was determined using a raw waveform. An optimal method for obtaining high-resolution energy spectrum was proposed. In order to correct the destructive effect of pile-up events in the energy spectrum, a new method based on maximum likelihood estimation was developed. Moreover, the Gaussian model function for the anode pulses directly emitted from the NaI detector (i.e., without using a preamplifier unit) was introduced and the performance of the proposed fast-fitting Gaussian method was investigated for the gamma-ray spectroscopy of a Cs-137 source. Also, a method based on FWHM determination has been introduced (rejection method 2). Finally, the pile-up rejection methods were studied.

2. Materials and methods

A Bicron 2" × 2″ NaI(Tl) scintillation detector and a PHOTONIS XP2020 PMT in tandem were used for the gamma-ray spectroscopy. Detector and digitizer system configurations are the same as in our previous work (Kasani et al., 2021). For the analog gamma-ray spectroscopy, a charge-sensitive preamplifier (ORTEC model 113) with the input capacitance of 200 nF, a main amplifier for pulse shaping and amplifying (ORTEC model 485), and an ADC/MCA instrument (ORTEC model 6240) were used.

2.1. Pulse arrival time

The techniques for achieving optimum timing resolution depend on detector type. Therefore, the correct timing discriminator must be chosen to match the characteristics of the detector. The leading-edge timing will give the best time resolution for pulses with a limited dynamic range of amplitudes. However, for pulses with a large range of amplitudes, the leading-edge timing methods show a large time walk. Constant fraction timing methods are very effective at reducing amplitude walk when the pulse shape does not change. Scintillation detectors (such as NaI and CsI) produce pulses of fixed shape when a given type of radiation is involved (Knoll, 2010).

To determine the pulse arrival time in the PMT anode-driven waveform, a combination of the digital constant-fraction discrimination (DCFD) method and the enhanced sampling rate waveform (Monzó et al., 2009) was applied. The number of raw waveform samples is increased L times higher than the original value by inserting L-1 zero samples between the two consecutive ones., as is shown in Equation (1).

$$z(n) = \begin{cases} x\left(\frac{n}{L}\right) & \text{n} = 0, \text{L}, 2\text{l}, \ldots \\ 0, & \text{elsewhere} \end{cases} \quad (1)$$

where x and z correspond to the original and the output waveforms respectively. On the next step, a fifth-order Butterworth low-pass filter with a cut-off frequency of 1/2L was used to obtain the enhanced sampling rate waveforms which increased the number of samples by L.

The constant-fraction discrimination (CFD) is well-known in analog timing measurements and its digital equivalent has been also introduced in different works (Fallu-Labruyere et al., 2007). The DCFD signal is described in Eq. (2):

$$y[i] = F.(x[i] - BSL) - (x[i + \Delta] - BSL) \quad (2)$$

where x, F, BSL, and Δ are the input waveform signal, the constant fraction, the baseline of the waveform signal, and the number of delayed samples, respectively. The BSL value can be reduced to zero either by averaging over a few sample pulses before the main pulse arrival or by using a high-pass filter with an appropriate cut-off frequency. In this work, the pre-set values of DCFD method parameters were F = 0.98, Δ = 6, and BSL = 0 for enhanced sampling rate waveforms.

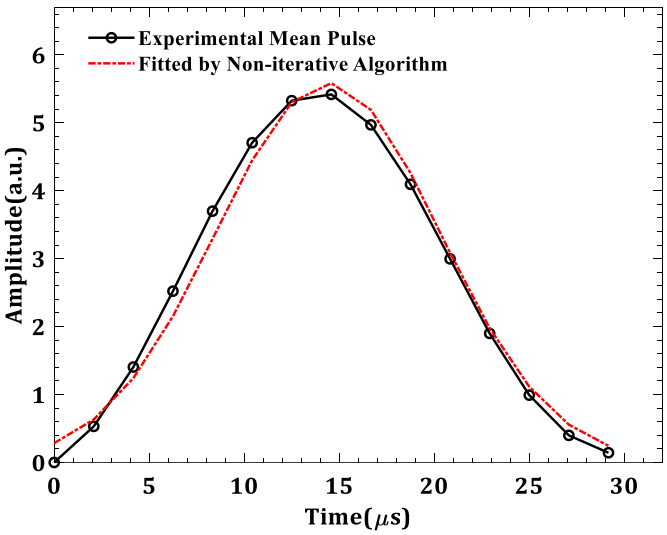

Fig. 1. Mean template pulse of gamma-ray pile-up-free PMT anode pulses digitized by PC sound card.

Table 1
Mean and standard deviation values of fitting parameters.

Fitting Parameter	Calculated Value
M	8.0 ± 0.8
Σ	2.4 ± 0.5

2.2. Pulse model

Several models have been proposed to describe the scintillation pulses, based on the scintillation process and photoelectron conversion physics. The most common models are the single-exponential and bi-exponential functions (Knoll, 2010). The Gaussian function (Equation (3)) can also be a rough approximation to the PMT anode current pulse.

$$f(x) = A \exp\left(-\frac{(x-\mu)^2}{2\sigma^2}\right) \quad (3)$$

where A, μ, and σ are the height, the peak position, and the control parameter of the Gaussian pulse width, respectively. The template pulse for the enhanced sampling rate waveform with L = 5 is shown in Fig. 1, obtained by averaging over 100 pile-up free pulses.

The σ and μ coefficients are listed in Table 1. The values were obtained by averaging over separate fittings on 100 pile-up-free pulses with standard deviation values as fitting errors.

2.2.1. Gaussian fast-fit method: non-iterative algorithm

Several methods for fast-fitting the Gaussian function on experimental data can be found in the literature (Caruana et al., 1986; Guo, 2011). In this study, a method was developed based on the Gaussian model with a polynomial function background (Roonizi, 2013) for the fitting of the Gaussian function. The derivative of the Gaussian model function is shown in Equation (4).

$$\frac{\partial f(x)}{\partial x} = -\frac{1}{\sigma^2} x f(x) + \frac{\mu}{\sigma^2} f(x) \quad (4)$$

By the integration of both sides of Eq. (4), one may obtain Eq. (5):

$$f(x) = -\frac{1}{\sigma^2}\int_0^x uf(u)du + \frac{\mu}{\sigma^2}\int_0^x f(u)du = \beta_1\varphi_1(x) + \beta_2\varphi_2(x) \tag{5}$$

where $\beta_1 = -1/\sigma^2$, $\beta_2 = \mu/\sigma^2$ and $\varphi_{1,2}(x)$ functions are the first and second integral terms, respectively. The error function is defined in Equation (6).

$$e(x) = f(x) - \sum_{k=1}^{2}\beta_k\varphi_k(x) \tag{6}$$

The cost function is also defined in Equation (7).

$$\xi = \int_{-\infty}^{+\infty}|e(x)|^2dx \tag{7}$$

By minimizing the cost function (or error function), the Gaussian function exhibits a good fitting with the experimental pulse function. Therefore, using the conditions $\partial\xi/\partial\beta_{1,2} = 0$, the researchers calculated the two unknown coefficients of σ and μ, by solving the two equations simultaneously. Finally, A as the height of the Gaussian pulse function was achievable by calculating the coefficients σ and μ, using the corresponding cost function minimization (Roonizi, 2013), as is presented in Equation (8).

$$A = \frac{\int_{-\infty}^{+\infty} f(x)\exp\left(-\frac{(x-\mu)^2}{2\sigma^2}\right)dx}{\left(\int_{-\infty}^{+\infty}\exp\left(-\frac{(x-\mu)^2}{2\sigma^2}\right)dx\right)^2} \tag{8}$$

Note should be taken that, the integrations above were converted into summations in discrete space.

2.3. Pile-up correction

2.3.1. Maximum likelihood estimation (MLE)

Pile-up events are nuisance in gamma-ray spectroscopy. A pile-up rejection method based on the pulse area correction was introduced in this study. An advantage of the MLE pile-up correction method (Ehrenberg et al., 1978) was its capability to select different pulse model functions. In this method, a model for the waveform was identified as follows:

$$r(x) = \sum_{i=1}^{N}A_i s(x-\tau_i) + n(x) \tag{9}$$

w here A_i, τ_i, and N are the height, pulse arrival time, and the total number of waveform pulses, respectively. Also, n(x) is related to the noise. Here, the *s(x)* is given as follows:

$$s(x) = \exp\left(-\frac{(x-\mu)^2}{2\sigma^2}\right) \tag{10}$$

where σ and μ are obtained from the fitting results of 100 pile-up-free pulses. They are used as constant values in Eq. (10). The actual height of the pulses was estimated by the matrix form of Eq. (11) in the MLE method:

$$A = \Lambda^{-1}\Phi \tag{11}$$

where the A matrix elements are the actual height of the pulses with the length of N, and the Λ matrix by the size of $N \times N$ is described as follows:

Fig. 2. Matrix elements corresponding to the first right and left (1st), etc. neighbors to each pulse.

$$\Lambda = \begin{bmatrix} \lambda_{11} & \lambda_{12} & \cdots & \lambda_{1N} \\ \cdots & & & \\ \lambda_{N1} & \lambda_{N2} & \cdots & \lambda_{NN} \end{bmatrix} \tag{12}$$

The values of the Λ matrix elements are specified by Eq. (13):

$$\lambda_{ij} = \int_0^T s(x-\tau_{0i})s(x-\tau_{0j})dx \tag{13}$$

where, the integration range is on the whole waveform, with N as the total number of samples. Each model function corresponded to the individual pulse arrival time, with the length equal to the whole waveform matrix which was prepared. The product of the *ith* and *jth* pulses was the multiplication of the corresponding elements in two pulses. Therefore, the product result had non-zero values only in the overlapped regions of the pulses. After calculating the product, the sum of the elements of the product matrix in the discrete space resulted in the elements of the λ_{ij} matrix. The matrix related to the corrected pulse heights can also be calculated by Eq. (14),

$$\Phi = \left[\int_0^T r(x)s(x-\tau_{01})dx, \ldots, \int_0^T r(x)s(x-\tau_{0N})dx\right] \tag{14}$$

where r (x) is the waveform collected from the PMT anode.

2.3.2. Proposed method

The run time dramatically increased in obtaining the matrix elements of Eq. (12), when the length of the collected waveform was too large (i.e., there were numerous presented pulses in the waveform). In this work, to reduce the run time, a new method was proposed by calculating the nearest-neighbor elements. The matrix fixed the main diagonal elements which avoided their recalculations.

As shown in Fig. 2, the run time can be significantly reduced by calculating the matrix elements of the nearest neighbors. The matrix elements related to the *rth* neighbor, on the right neighbor to each pulse, can be calculated by Eq. (15), as follows:

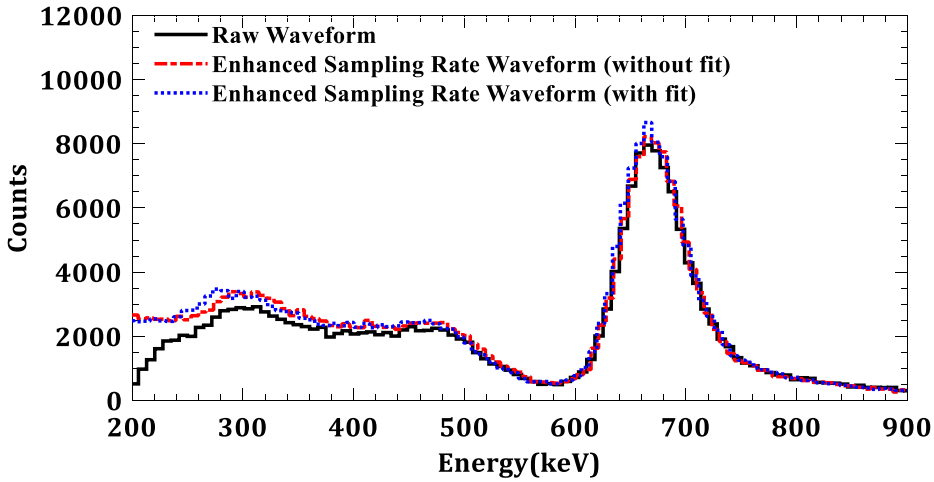

Fig. 3. Experimental spectra obtained by different proposed methods for extraction of gamma-ray energy from anode pulses digitized in 96 kHz.

Table 2
Corresponding count rates in various source distances from the NaI detector.

Source-to-detector distance (cm)	4	2	0
Count Rate (kcps)	5.3	8.6	13.4

$$\lambda_r^{(k)} = \sum_{n=1}^{N-r} s(x_{0n})s(x_{0n+r}), \quad k = 1, 2, ..., N-r \tag{15}$$

where N is the total number of pulses in the waveform. Also, the matrix elements related to the left neighbor to each pulse can be calculated by Eq. (16), as follows:

$$\lambda_\ell^{(k)} = \sum_{n=\ell+1}^{N} s(x_{0n})s(x_{0n-\ell}), \quad k = 1, 2, ..., N-\ell \tag{16}$$

As shown in Fig. 2, the matrix elements corresponding to the right neighbors have r = 1, and the left neighbors have $l = 1$. Also, the matrix relation (13) should be obtained symmetrically in order to apply to n close neighbors. In other words, both the related terms to n neighbors on the right (Eq. (15)) and the n neighbors on the left (Eq. (16)) must be considered simultaneously, and the matrix is not only an upper or lower triangular matrix.

3. Results and discussion

The energy information can be obtained from the raw waveform, without using the algorithms to increase the waveform sampling rate. To this end, various algorithms were applied to detect the pulse arrival time in the raw waveform, but they were proved unsuccessful. In this study, a method was proposed to detect the index of peak time (n) for each pulse, by setting the pulse arrival time index to (n-1). The energy of each pulse was obtained by considering the pulse length of 3 samples and the sum of the corresponding heights (Black solid line in Fig. 3).

In the next step, the number of waveform samples was increased by the method described in the previous section, and the pulses in the new waveform were separated, by using the DCFD method before storing in a two-dimensional matrix array. It should be noted that the lower L value resulted in a lower run time, meanwhile, the optimal L value was obtained. By examining different L values, the researchers reached the optimal value of 5 for this parameter. Therefore, all subsequent calculations, including the appropriate algorithm for determining the pulse arrival time, were set up on L = 5. Two strategies were employed to obtain the pulse area (or, the corresponding gamma-ray energy); (1) the direct summation of the values for each experimental pulse (Red dashed line in Fig. 3), and (2) the summation of the values for the Gaussian function fitted pulse on that pulse (Blue dot line in Fig. 3).

Table 3
A summary of the obtained energy resolution measurement results from three digital methods.

	Energy Resolution (%)		
Count Rate (kcps) → Method ↓	5.3	8.6	13.4
Raw Waveform	7.9 ± 0.6	9.9 ± 0.6	18.9 ± 0.8
Enhanced Sampling Rate Waveform (without fit)	7.5 ± 0.6	9.4 ± 0.6	15.8 ± 1.3
Enhanced Sampling Rate Waveform (with fit)	7.2 ± 0.6	9.0 ± 0.7	14.6 ± 0.4

The calculations for obtaining the energy spectra of Fig. 3 were performed at a count rate of 5.3 kcps. Table 2 summarizes the count rates at different detector distances from the source. As mentioned, gamma-ray spectroscopy was performed, using the raw waveform and enhanced sampling rate waveform. The performance of the methods was evaluated by the capability of high energy resolution achievement at different count rates. An investigation was carried out on the energy calibration of spectra.

The calibration was performed using linear fitting of full-energy (662 keV), and Compton edge (478 keV) peaks. The energy resolution was obtained, by calculating photopeak FWHM in calibrated spectra and dividing its value by the corresponding energy (662 keV). The FWHM values were obtained by the Multiple Peak Fit module of ORIGIN data analysis software. The standard deviation value was also given as an output of the software.

Table 3 represents the results of the energy resolution values at different counts for the spectra, obtained from the raw waveform and the enhanced sampling rate waveform (i.e., the pulse area calculation, with/without using the model function fitting). As can be seen in Table 3, the energy resolution was lower when the number of samples increased. The pulse area was obtained by a non-iterative Gaussian function fitting algorithm.

Despite the small number of samples per pulse, the researchers used the enhanced sampling rate waveform and MLE method to correct the destructive effect of pile-up events on the energy spectrum. Fig. 4 represented corrected and uncorrected energy spectrum at different count rates.

The model function used in the MLE method was Eq. (10), in which the fitting parameters were constant (Table 1). The main issue was the extremely high run time of the MLE method for large waveforms. To reduce the run time of the MLE algorithm, which corrected the

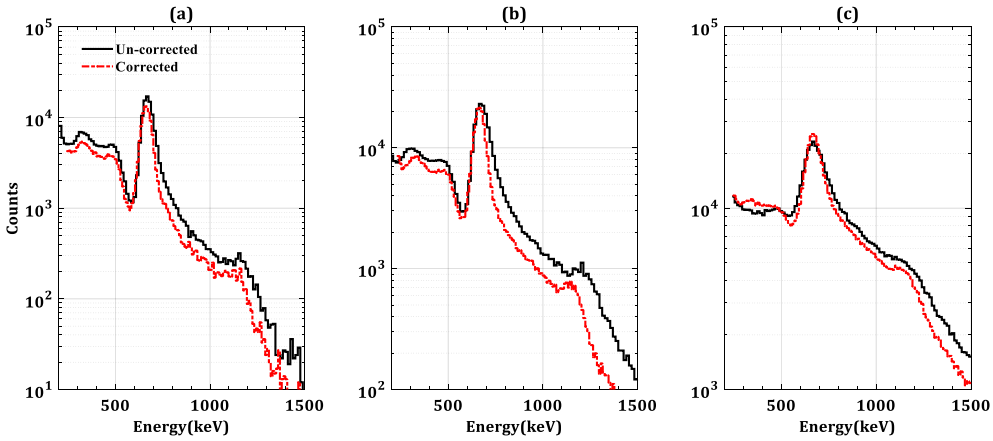

Fig. 4. Experimental corrected and uncorrected spectra at count rates of (a) 5.3, (b) 8.6, and (c) 13.4 kcps. (No Figure???).

Table 4
Energy resolution results of an NaI (Tl) scintillator with and without the pile-up correction.

Count Rate (kcps)	Energy Resolution (%)	
	Uncorrected	Corrected
5.3	7.2 ± 0.6	7.8 ± 0.3
8.6	9.0 ± 0.7	7.7 ± 0.5
13.4	14.6 ± 0.4	11.5 ± 0.4

destructive effect of pile-up events on the energy spectrum, a method was proposed by considering the contribution of nearest neighbors to each pulse in the calculation. To determine the number of neighbors to be considered in different count rates, the researchers implemented the proposed approximate method, starting from the nearest to the furthest neighbor. The results of the MLE method were precisely consistent with the results obtained from the approximate method, by considering only one neighbor in all three count rates. Table 4 summarizes the results of energy resolution with/without the pile-up correction. As it can be seen, after the pile-up correction, the energy resolution had no significant improvement at low count rates; whereas the energy resolution was effectively improved at high count rates.

Due to the low sampling rate, the probability of detecting pile-up events decreased, since only one detectable close neighbor could stay on the tail of the first pulse. The proposed method could locate undetectable pulses under a pile-up event, relying on the stability of the output pulse from the PMT anode. Undoubtedly, such events as electronic noises could have deformed the stability of the PMT output pulse and gave subsequent inaccurate information about the incoming gamma-ray energy. In this method, a pulse of full width at half maximum (FWHM) in a certain range was assumed as a pile-up-free pulse. To reach the acceptable range of FWHM, the FWHM of all pulses in the waveform was obtained by fitting the Gaussian function to the

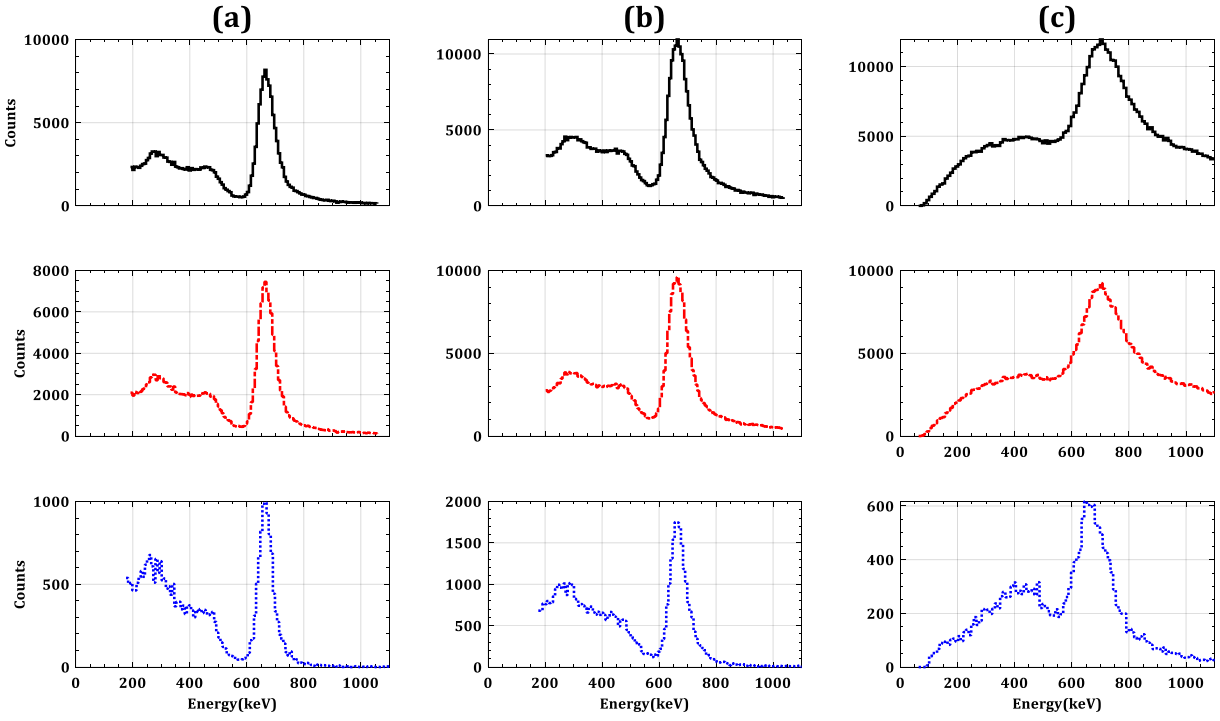

Fig. 5. Measured spectra without pile-up rejection (black solid line), with pile-up rejection using the method I (red dash line) and using method II (blue dot line) at different count rates with corresponding count rate values in curve columns of (a) 5.3, (b) 8.6 and (c) 13.4 kcps. (For interpretation of the references to colour in this figure legend, the reader is referred to the Web version of this article.)

Table 5
Energy resolution data for rejection of the pile-up events by two different methods.

Count Rate (kcps)	Energy resolution (%)			Relative Peak Height (%)	
	Without rejection	Rejection method 1	Rejection method 2	Rejection method 1	Rejection method 2
5.3	7.2 ± 0.6	7.1 ± 0.5	6.2 ± 0.5	91.1	12.1
8.6	9.0 ± 0.7	8.9 ± 0.6	6.9 ± 0.9	87.6	15.9
13.4	14.6 ± 0.4	14.4 ± 0.6	13.0 ± 0.9	77.3	5.2

experimental pulses (FWHM≃2.355σ), at low count rates. Given the high probability of pile-up-free events at low count rates, the range of the highest amplitude in the histogram of FWHMs was the rational and desirable range for FWHMs.

Two methods were employed to reject pile-up events. In the first method, a staying pulse on the tail of the preceding pulse was rejected, by obtaining the index of the arrival time of pulses in waveforms. The energy of the pulse was removed, only if the interval time of a given pulse from the former was less than the average pulse length (i.e., 13 samples for enhanced sampling rate waveforms). In the second method, both neighboring pulses and the ones with FWHM of the non-acceptable range were omitted. Fig. 5 shows the results of rejecting the pile-up events, by using methods 1 and 2 at different count rates.

The quantitative results for the energy resolution at different count rates and the two employed methods are listed in Table 5. As it can be seen, the energy resolution was improved by eliminating the pile-up events. In particular, the second method contributed immensely to the improvement. Also, Table 5 shows the ratio of the height of the photopeak, before/after rejecting the pile-up events, which corresponded to the number of omitted events at three different count rates.

As it can be seen, the widths of a large number of pulses increased by the pile-up event. As it is impossible to correct those types of pulses, the researchers eliminated their contributions to the energy spectrum. Finally, we obtained an energy resolution of 6.8% for all count rates, which was measured by the conventional analog method. The setup configuration of the analog method is described in Section 2.

4. Conclusions

Digital gamma-ray spectroscopy was performed, by adopting a low-cost and publicly available digitizer (Commercial off the shelf) (a PC sound card) and direct digitization of the output pulses of the NaI(Tl) PMT anode. The gamma-ray spectroscopy of the Cs-137 source was performed, using raw waveforms as well as enhanced sampling rate waveforms. By employing a digital constant fraction discrimination (DCFD) method, the researchers obtained the arrival time of pulses by increasing the sampling rate of waveforms. Also, the related energy (pulse area) of each pulse was obtained by direct summing values of each pulse sample, and values of pulse samples fitted by the Gaussian model function. Results proved that the high energy resolution achievement could be obtained, by using increased sampling rate waveforms and the Gaussian model function fitting to calculate energy.

Correction of pile-up events at different count rates was performed, by the Maximum Likelihood Estimation (MLE) method. To reduce the run time, the researchers introduced an approximation method to adapt the MLE method. Accordingly, it was found that only one close neighbor to a given pulse stays on the tail of the former pulse (i.e., pile-up event). The energy resolution of photopeak was improved after the correction of the pile-up events at different count rates. Two methods were implemented to reject the pile-up events. The results showed that the second method was more favorable to high-resolution achievements. Furthermore, in the second method, the number of the rejected events was bigger than the first method. The rejection of the pile-up events by the second method increased the energy resolution of the 662 keV gamma-rays to 6.2%.

Declaration of competing interest

The authors declare that they have no known competing financial interests or personal relationships that could have appeared to influence the work reported in this paper.

Acknowledgments

The project has been supported by a research grant from the University of Tabriz (№ SAD/3/14000115).

References

Buzzetti, S., Capou, M., Guazzoni, C., Longoni, A., Mariani, R., Moser, S., 2005. High-speed FPGA-based pulse-height analyzer for high resolution X-ray spectroscopy. IEEE Trans. Nucl. Sci. 52, 854–860.
Caruana, R.A., Searle, R.B., Heller, T., Shupack, S.I., 1986. Fast algorithm for the resolution of spectra. Anal. Chem. 58, 1162–1167.
Ehrenberg, J., Ewart, T., Morris, R., 1978. Signal-processing techniques for resolving individual pulses in a multipath signal. J. Acoust. Soc. Am. 63, 1861–1865.
Fallu-Labruyere, A., Tan, H., Hennig, W., Warburton, W., 2007. Time resolution studies using digital constant fraction discrimination. Nucl. Instrum. Methods Phys. Res. Sect. A Accel. Spectrom. Detect. Assoc. Equip. 579, 247–251.
Guo, H., 2011. A simple algorithm for fitting a Gaussian function [DSP tips and tricks]. IEEE Signal Process. Mag. 28, 134–137.
Huang, Q., Jiang, J., 2018. A radiation-tolerant wireless monitoring system using a redundant architecture and diversified commercial off-the-shelf components. IEEE Trans. Nucl. Sci. 65, 2582–2592.
Kasani, H., Ashrafi, S., Ghal-Eh, N., 2021. High count-rate digital gamma-ray spectroscopy using a low-cost COTS digitizer system. Radiat. Phys. Chem. 184, 109438.
Kinahan, P.E., Karp, J.S., 1990. Position estimation and error correction in a 2D position-sensitive NaI (Tl) detector. Nucl. Instrum. Methods Phys. Res. Sect. A Accel. Spectrom. Detect. Assoc. Equip. 299, 484–489.
Knoll, G.F., 2010. Radiation Detection and Measurement. John Wiley & Sons.
Mantero, J., Gázquez, M., Hurtado, S., Bolívar, J., García-Tenorio, R., 2015. Application of gamma-ray spectrometry in a NORM industry for its radiometrical characterization. Radiat. Phys. Chem. 116, 78–81.
Mohammadian-Behbahani, M.-R., Saramad, S., 2020. A comparison study of the pile-up correction algorithms. Nucl. Instrum. Methods Phys. Res. Sect. A Accel. Spectrom. Detect. Assoc. Equip. 951, 163013.
Monzó, J.M., Lerche, C.W., Martínez, J.D., Esteve, R., Toledo, J., Gadea, R., Colom, R.J., Herrero, V., Ferrando, N., Aliaga, R.J., 2009. Analysis of time resolution in a dual head LSO+ PSPMT PET system using low pass filter interpolation and digital constant fraction discriminator techniques. Nucl. Instrum. Methods Phys. Res. Sect. A Accel. Spectrom. Detect. Assoc. Equip. 604, 347–350.
Roonizi, E.K., 2013. A new algorithm for fitting a Gaussian function riding on the polynomial background. IEEE Signal Process. Lett. 20, 1062–1065.